ARTICLE

OPEN ACCESS

www.the-innovation.org

Global trends and regime state shifts of lacustrine aquatic vegetation

Juhua Luo,[1,2] Hongtao Duan,[1,2,*] Ying Xu,[1,2] Ming Shen,[1] Yunlin Zhang,[1,2,*] Qitao Xiao,[1] Guigao Ni,[1] Kang Wang,[1] Yihao Xin,[1,2] Tianci Qi,[1] Lian Feng,[3] Yinguo Qiu,[1] Erik Jeppesen,[4,5,6] and R. Iestyn Woolway[7]

*Correspondence: htduan@niglas.ac.cn (H.D.); ylzhang@niglas.ac.cn (Y.Z.)

Received: April 17, 2024; Accepted: December 30, 2024; Published Online: January 2, 2025; https://doi.org/10.1016/j.xinn.2024.100784

GRAPHICAL ABSTRACT

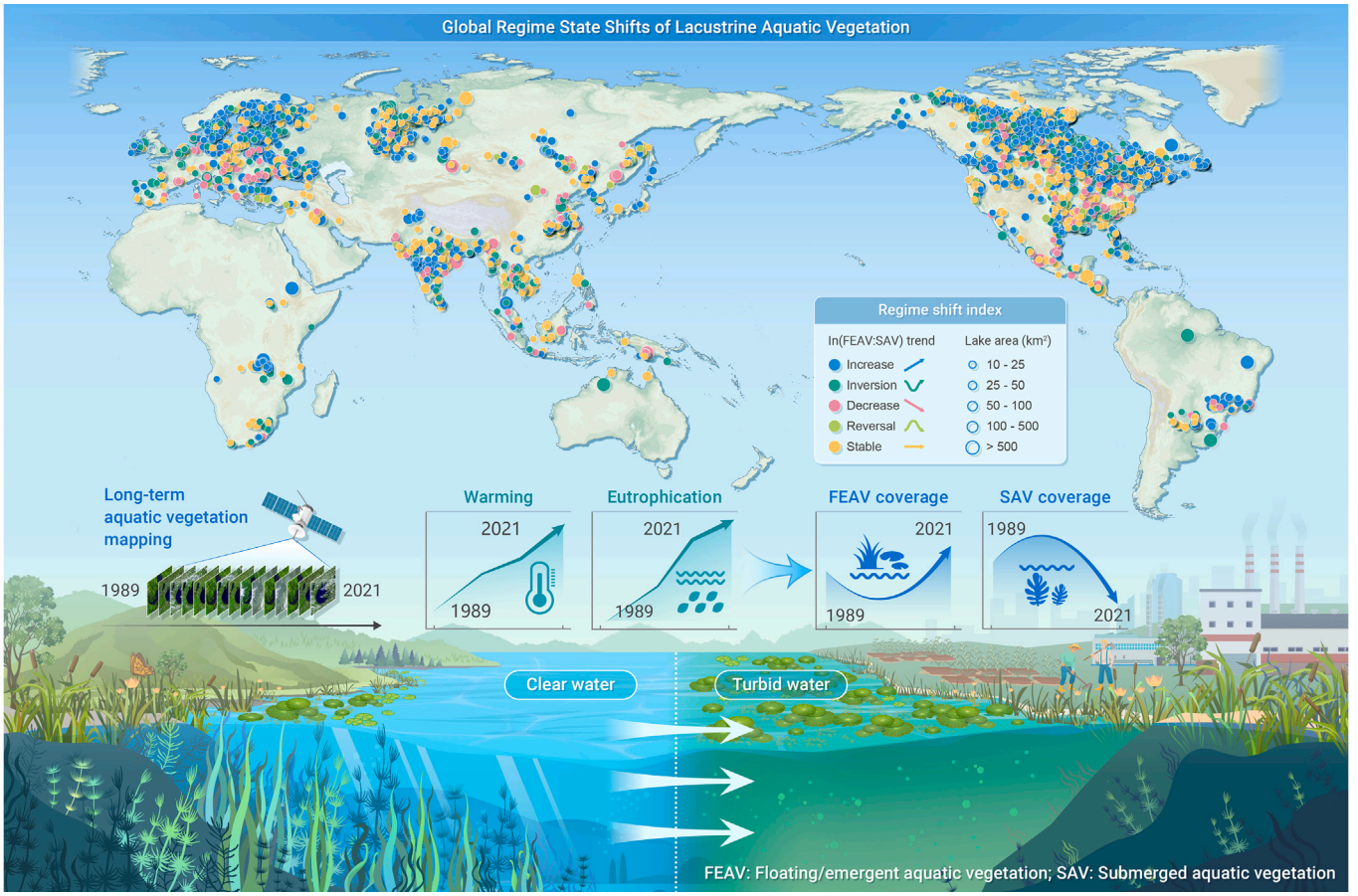

PUBLIC SUMMARY

- A global database (1989–2021) of lacustrine aquatic vegetation was established.
- Submerged vegetation has declined rapidly, whereas floating and emergent vegetation increased slightly.
- The global trend in aquatic vegetation indicates a potential shift toward states characterized by increased shading and turbidity.
- Human activities primarily drove changes in lakes until the early 2010s, but climate warming has since become a dominant driver.

OPEN ACCESS

ARTICLE

The Innovation

Global trends and regime state shifts of lacustrine aquatic vegetation

Juhua Luo,[1,2] Hongtao Duan,[1,2,*] Ying Xu,[1,2] Ming Shen,[1] Yunlin Zhang,[1,2,*] Qitao Xiao,[1] Guigao Ni,[1] Kang Wang,[1] Yihao Xin,[1,2] Tianci Qi,[1] Lian Feng,[3] Yinguo Qiu,[1] Erik Jeppesen,[4,5,6] and R. Iestyn Woolway[7]

[1]Key Laboratory of Lake and Watershed Science for Water Security, Nanjing Institute of Geography and Limnology, Chinese Academy of Sciences, Nanjing 210008, China
[2]University of Chinese Academy of Sciences, Nanjing (UCASNJ), Nanjing 211135, China
[3]School of Environmental Science and Engineering, Southern University of Science and Technology, Shenzhen 518055, China
[4]Limnology Laboratory, Department of Biology, Middle East Technical University, Ankara 06800, Türkiye
[5]Department of Ecoscience and Center for Water Technology (WATEC), Aarhus University, 8000 Aarhus, Denmark
[6]Institute for Ecological Research and Pollution Control of Plateau Lakes, School of Ecology and Environmental Science, Yunnan University, Kunming 650500, China
[7]School of Ocean Sciences, Bangor University, Bangor LL57 2DG, UK
*Correspondence: htduan@niglas.ac.cn (H.D.); ylzhang@niglas.ac.cn (Y.Z.)

Received: April 17, 2024; Accepted: December 30, 2024; Published Online: January 2, 2025; https://doi.org/10.1016/j.xinn.2024.100784

Citation: Luo J., Duan H., Xu Y., et al., (2025). Global trends and regime state shifts of lacustrine aquatic vegetation. The Innovation **6(3)**, 100784.

Aquatic vegetation (AV) is vital for maintaining the health of lake ecosystems, with submerged aquatic vegetation (SAV) and floating/emergent aquatic vegetation (FEAV) representing clear and shaded states, respectively. However, global SAV and FEAV dynamics are poorly understood due to data scarcity. To address this gap, we developed an innovative AV mapping algorithm and workflow using satellite imagery (1.4 million Landsat images) from 1989 to 2021 and created a global database of AV across 5,587 shallow lakes. Our findings suggest that AV covers 108,186 km^2 on average globally, accounting for 28.9% (FEAV, 15.8%; SAV, 13.1%) of the total lake area. Over two decades, we observed a notable transition: SAV decreased by 30.4%, while FEAV increased by 15.6%, leading to a substantial net loss of AV. This global trend indicates a shift from clear to shaded conditions, increasingly progressing toward turbid states dominated by phytoplankton. We found that human-induced eutrophication was the primary driver of change until the early 2010s, after which global warming and rising lake temperatures became the dominant drivers. These trends serve as a warning sign of deteriorating lake health worldwide. With future climate warming and intensified eutrophication, these ongoing trends pose a significant risk of disrupting lake ecosystems.

INTRODUCTION

Aquatic vegetation (AV), comprising submerged AV (SAV) and floating/emergent AV (FEAV), is essential for maintaining the health of lake ecosystems. As primary producers, they contribute to carbon sequestration and have significant influence on biodiversity preservation and water quality.[1–4] SAV and FEAV provide distinct ecological effects. SAV enhances water clarity through positive feedback mechanisms such as reduced sediment resuspension and increased zooplankton grazing on phytoplankton.[1,5–7] In contrast, FEAV, particularly dense free-floating vegetation, hinders light penetration, creates dense shade, and negatively affects underwater organisms.[8–10] Thus, they represent two alternative regimes: a clear state dominated by SAV and a shaded state dominated by FEAV.[10–13] The clear SAV-dominated state is characterized by low turbidity, intermediate abundance of phytoplankton, high coverage of SAV, and absence of small floating macrophytes.[10] In contrast, the shaded state is characterized by high turbidity, high abundance of phytoplankton, absence of SAV, and high coverage of small floating macrophytes.[10,13] The decline or disappearance of SAV and the expansion or invasion of FEAV can trigger significant regime shifts from a clear SAV-dominated to a shaded FEAV-dominated state.[8,10] Shifts in primary producers have implications for key ecosystem services provided by lakes, including supporting, provisioning, regulating, and cultural services.[11,12,14] Therefore, understanding the spatiotemporal changes in SAV and FEAV is critical for detecting regime state shifts and major changes in ecosystem functions.

In recent decades, global lake ecosystems have undergone substantial changes due to human activities and climate change, including increased eutrophication and more frequent occurrences of algal bloom (AB).[15–17] However, our understanding of global SAV and FEAV dynamics, as well as the potential regime shifts in lacustrine AV, remains limited. This knowledge gap primarily stems from limited field observations, characterized by insufficient temporal and spatial coverage. To address these limitations, satellite remote sensing has emerged as an effective method for detecting and tracking AV distribution and changes at large spatial scales.[18–20] However, global-scale studies examining the different communities of AV (i.e., SAV and FEAV) in lakes remain scarce. In this study, we aim to fill this knowledge gap using remote sensing to address three key questions. (1) What is the global distribution of lacustrine AV, including SAV and FEAV communities, and where are these communities located? (2) How have these distributions changed since the advent of large-scale satellite data in the 1980s? (3) What are the underlying drivers or mechanisms behind these changes?

MATERIALS AND METHODS

Data sources

We used Landsat-5 Thematic Mapper (TM) and Landsat-8 Operational Land Imager (OLI) surface reflectance products (LANDSAT/LT05/C01/T1_SR and LANDSAT/LC08/C01/T1_SR) obtained from Google Earth Engine (GEE) to map global lacustrine AV from 1989 to 2021. The Landsat satellites provide 30-m spatial resolution in the optical bands with a 16-day revisit cycle. Each scene includes a quality assessment band, which we coupled with the Fmask algorithm to effectively remove cloud cover, cloud shadow, and other contaminated pixels.

We delineated the study lakes using lake vectors provided by HydroLAKES (v.1.0).[21] For lakes in China, we employed vector boundaries from the "China Lake Survey Dataset."[22] To exclude karst and saline lakes, we utilized vector boundaries for inland basins from Wang et al.[23] High-latitude lakes were excluded using the "skin_temperature" band from the "ERA5-Land Monthly Aggregated" data available on GEE. To identify the key global drivers of AV, we obtained country-level data on pesticide usage (1990–2021), inorganic fertilizer usage (1989–2021), impervious surface data (1992–2021), and land surface temperature (LST) changes (1989–2021) from the Food and Agriculture Organization (FAO).

Creation of a global lacustrine AV database

We developed a global AV database covering both FEAV and SAV. The creation of this database involved four key steps (Figure 1; see detailed information in the supplemental text). Step 1 was selection of study lakes. Lakes with a surface area <10 km^2 and an average depth >15 m were excluded. Additionally, lakes in high-latitude and endorheic basins were masked to reduce uncertainties, resulting in a focus on 6,948 relatively shallow lakes.[23] Step 2 was image selection and processing. Landsat 5 and 8 images with a 30-m resolution were selected for the critical growing seasons for AV, covering the period from 1989 to 2021. In total, 1.4 million images were selected, with cloud and ice pixels removed. Step 3 was use of the automated vegetation and bloom indices (VBI) algorithm for mapping FEAV and SAV. VBI was used to classify the pre-processed images into four categories: AB, open water (OW), FEAV, and SAV.[19] This method, developed previously, was executed on the GEE platform. Step 4 was calculation of the areas of AV, FEAV, and SAV. For each 2-year period, we calculated the maximum area covered by AV, FEAV, and SAV based on the classification maps. This resulted in a composite database comprising 16 data periods (1989–2021) per lake. Based on this database, we calculated the coverage of AV, SAV, and FEAV at local, regional, and global scales. Furthermore, from this database, we analyzed global patterns and trends in AV, SAV, and FEAV.

Validation and assessment

We extensively validated the classification maps and area data using 7,144 field samples from 49 lakes in China (Figure S1), achieving an overall accuracy of 87.4% (Tables S1 and S2). These field samples, collected through ground investigation and literature searches,

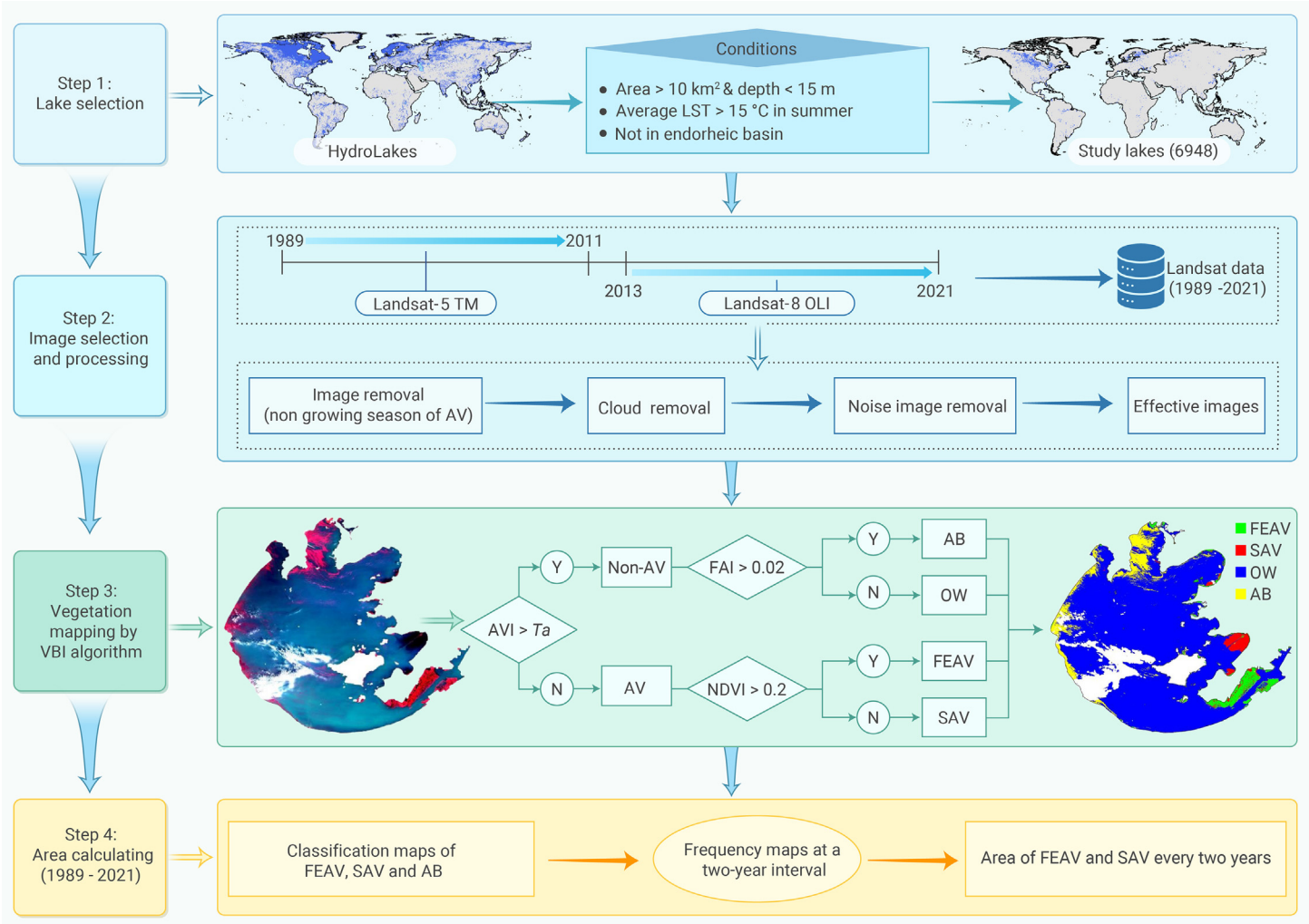

Figure 1. Practical workflow for constructing an AV database

covered the periods of 2008–2011 and 2018–2021. The mapping accuracy for SAV was 80.1% for the producer's accuracy and 81.4% for the user's accuracy. For FEAV, the mapping accuracy was 92.0% for the producer's accuracy and 88.5% for the user's accuracy (Table S2).

Due to limited global field data, we also thoroughly validated the AV classification, distribution, and trends with literature and high-resolution imagery. Our results were assessed using four methods.

(1) Comparative validation with published classification maps. We extracted the spatial distribution maps of AV in 13 lakes from the literature. By visually comparing our results with published classification maps, specifically focusing on the spatial distribution of FEAV and SAV, we found that our extraction results closely matched the documented extents (Figure 2).

(2) Qualitative assessment based on literature-derived AV information. We conducted AV monitoring for 14 lakes with records of AV groups or spatial distribution in the literature and qualitatively verified the results combined with remote sensing imagery (Figure S2). Our results confirm the accuracy of the classification maps.

(3) Change trend validation. To demonstrate the algorithm's robustness, we gathered long-term AV data from review articles by Botrel and Maranger[1] and Zhang et al.[24] and compared the reported trends. In 47 (77%) of the 61 lakes for which we gathered time-series data, the trends were consistent (Tables S3 and S4).

(4) Validation of SAV maps using high-resolution imagery and ground-truth photographs. We acquired field- and high-spatial-resolution images, including 0.1-m unmanned aerial vehicle (UAV) imagery, 0.7-m JL-1 satellite imagery, and 10-m Sentinel-2 satellite imagery for multiple lakes globally. These images were visually interpreted to delineate SAV distributions. Our analyses showed close agreement between the extracted SAV extents and actual vegetation patterns (Figure S3). For Lake Taihu, ground-truth photos and UAV images clearly demonstrate the effectiveness of Landsat in distinguishing the presence or absence of SAV (Figure S4).

The validation results demonstrated the feasibility of our method and the reliability of the data obtained.

Spatiotemporal patterns and changes

To ensure the reliability and effectiveness of the image data for analyzing spatiotemporal patterns and changes of AV, lakes with an average total observation count per pixel of less than 96 (less than three valid observations per pixel per year on average) were excluded (998 lakes). Meanwhile, lakes with fewer than 13 biennial time points (301 lakes) were excluded from long-term change analyses. Additionally, we identified occurrences of desiccation in 62 of the 72 study lakes in Oceania during the observation period, and these lakes were also excluded. Consequently, a total of 5,587 lakes globally were selected for analyzing spatiotemporal patterns of AV, SAV, and FEAV.

Vegetation coverage was used as an indicator to visualize the spatial distribution patterns of AV, SAV, and FEAV. This analysis encompassed vegetation coverage at multiple scales, including in individual lake and continental and global scales. For individual lakes, we calculated the average vegetation area during the specified period. At continental and global scales, we quantified the ratio of the combined vegetation area over a 30-year period to the total lake area. This ratio was used as the overall regional coverage to characterize the spatial patterns of AV coverage:

$$C_x = \frac{\sum_{i=1}^{k} A_{i,x}}{\sum_{i=1}^{k} A_{i,lake}}, \quad \text{(Equation 1)}$$

where x represents the vegetation type (i.e., AV, FEAV, or SAV), k is the number of study lakes, C_x is the average coverage of x globally from 1989 to 2021, $A_{i,x}$ represents the average area of x in lake i between 1989 and 2021, and $A_{i,lake}$ indicates the area of lake i.

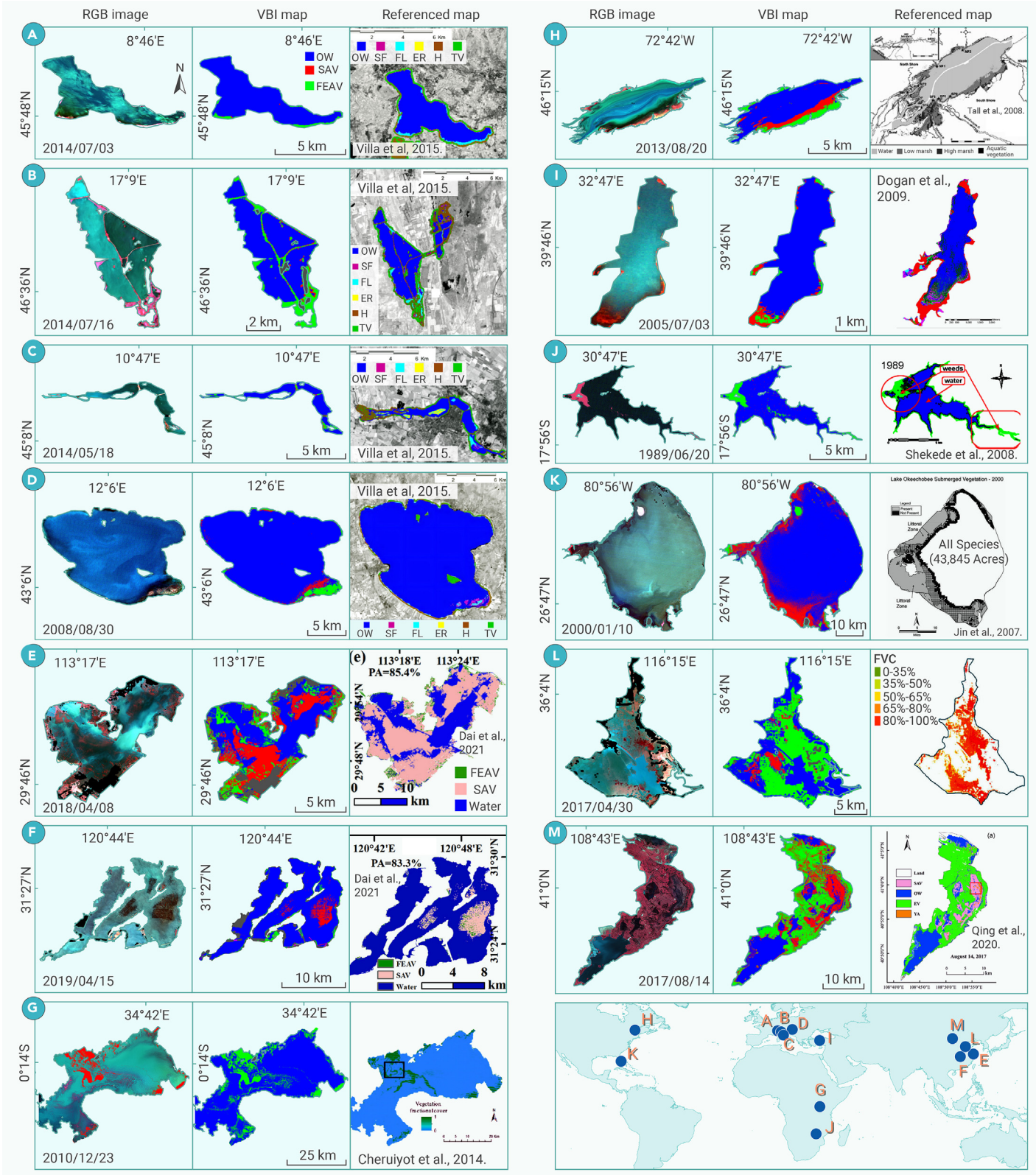

Figure 2. AV classification maps in 13 lakes globally by our VBI algorithm and from literature (A) Lake Varese, Italy. (B) Kis-Balaton wetland, Hungary. (C) Mantua Lakes system, Italy. (D), Lake Trasimeno, Italy. (E) Lake Honghu, China. (F) Lake Yangcheng, China. (G) Winam Gulf section of Lake Victoria, Uganda. (H) Lake Saint-Pierre, Canada. (I) Lake Mogan, Turkey. (J) Lake Chivero, Zimbabwe. (K) Lake Okeechobee, US. (L) Lake Dongping, China. (M) Lake Ulansuhai, China.

For individual lakes, vegetation coverage was quantified as the ratio of vegetation area to lake surface area. At continental and global scales, overall vegetation coverage was evaluated biennially to construct historical regional trends.

We analyzed the trends of FEAV and SAV by visually classifying them into five categories: increase, decrease, recovery, unimodal, and stable (Figure S5). These trend types were determined based on relevant studies and data analysis,[1] with a significance threshold of $p < 0.1$, assessed using a t test.

At continental and global scales, we initially fit a linear model to the coverage changes over the 16 periods within the region:

$$Y(t) = a_1 t + a_0, \quad \text{(Equation 2)}$$

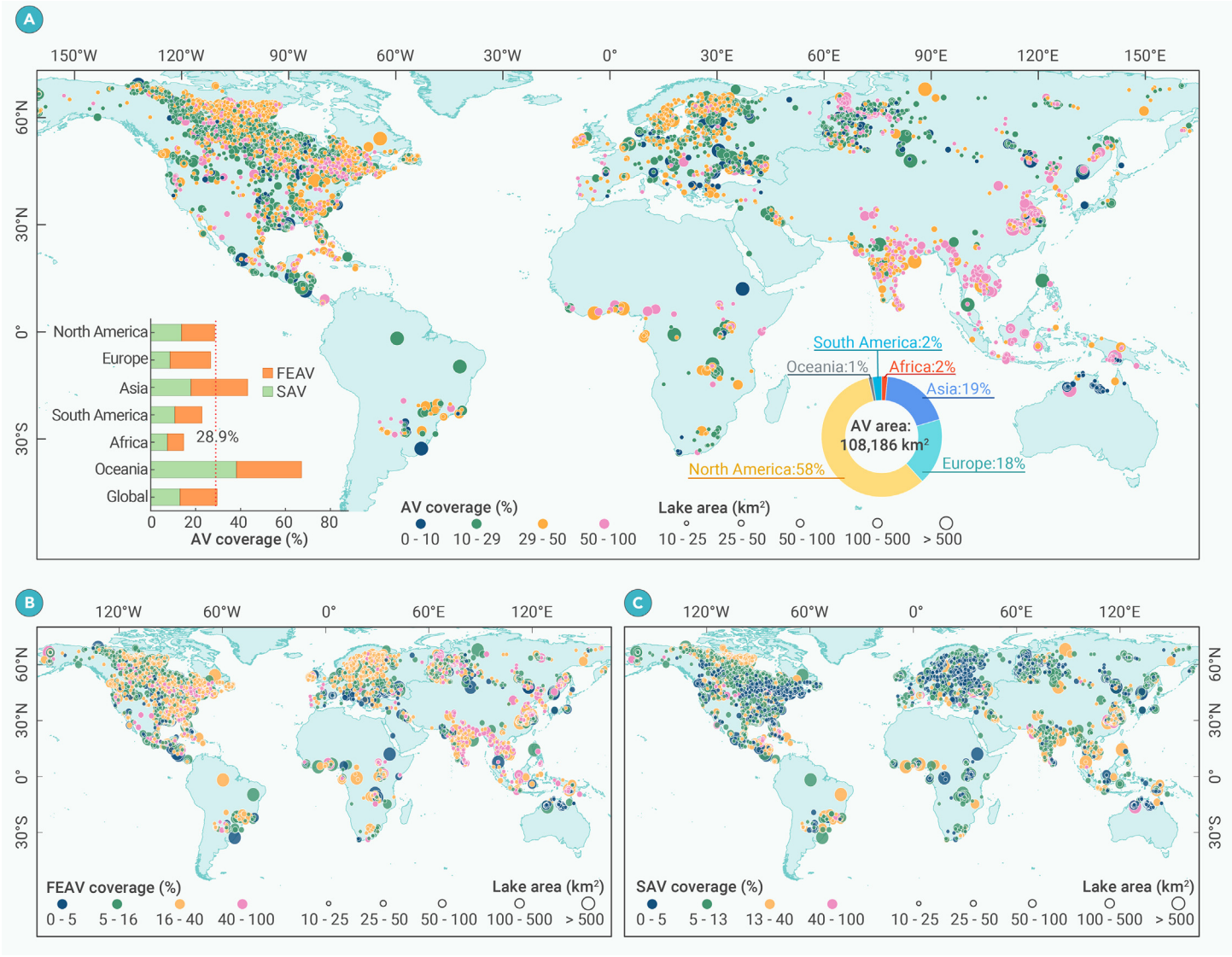

Figure 3. Global patterns of lacustrine AV coverage between 1989 and 2021 (A) Distribution of aquatic vegetation (AV) and percentage of AV coverage (average coverage area over 30 years relative to total lake area) at global and continental scales. (B) Coverage of floating/emergent AV (FEAV). (C) Coverage of submerged AV (SAV).

where Y represents the overall regional coverage of AV, t denotes time, and a_1, a_0 are regression coefficients determined through the principles of least squares.

If vegetation type in this region exhibits a linear change through a t test ($p < 0.1$), the changes were classified as "increase" ($a_1 > 0$) or "decrease" ($a_1 < 0$). If $p > 0.1$, then a quadratic fit was applied: trends with $p < 0.1$ for a_2 were classified as "universal" ($a_2 > 0$) or "inversion" ($a_2 < 0$) or otherwise as "stable":

$$Y(t) = a_2 t^2 + a_1 t + a_0, \quad \text{(Equation 3)}$$

where the coefficients a_0, a_1, and a_2 are regression coefficients.

To understand differences in vegetation coverage and surface area among lakes, annual coverage data for each lake were standardized as z scores using its own long-term mean and standard deviation.[15]

Regime state index

To explore the evolutionary patterns of AV communities, we constructed a regime state index (η) to analyze changes in FEAV and SAV coverage. η for each stage was calculated as follows: η = ln (FEAV:SAV), capturing long-term changes and reflecting the evolution of AV communities. During the analysis, we excluded single-period data with zero coverage of SAV. Then, we statistically analyzed the trends in η over 30 years for 5,572 lakes, ignoring time series with fewer than 13 periods of valid data (15 lakes). To understand the long-term evolution in global AV communities, we categorized the trend of η into five types: increase, inversion, decrease, reversal, and stable (Figure S5).

Furthermore, the critical years for each lake were identified based on the change analysis, including those corresponding to abrupt changes and points of accelerated increase in η. The Mann-Kendall abrupt test (M-K test) was used to detect abrupt changes, while Theil-Sen's slope analysis identified the accelerating rate of these changes. The year corresponding to the point of accelerated increase in η was calculated by fitting a secondary curve to the η series. Tangents were then drawn from both the year of the abrupt change in η and the final year to the fitted curve, with their intersection marking the year of accelerated increase. Following these steps, the critical years can be identified for individual lakes or across continents.

Analysis of natural and anthropogenic factors

The occurrence of the critical years in the evolution of lake AV is influenced by a combination of natural and anthropogenic factors. Using available data, we investigated the factors driving changes in AV, particularly the transition from the SAV to the FEAV regime state. By analyzing records from 3,385 lakes across 67 countries, we explored relationships between pesticide and inorganic fertilizer usage, impervious surface area, LST, and η. Based on the trend in η changes, the period from 1989 to 2021 is divided into three stages: 1989–2001, 2002–2010, and 2011–2021. We calculated the contributions using the Boruta R package to assess the impact of the four factors on η across the three stages. This package, based on the random forest algorithm, facilitates feature selection and detection of crucial features significantly correlated with the target variable.[25]

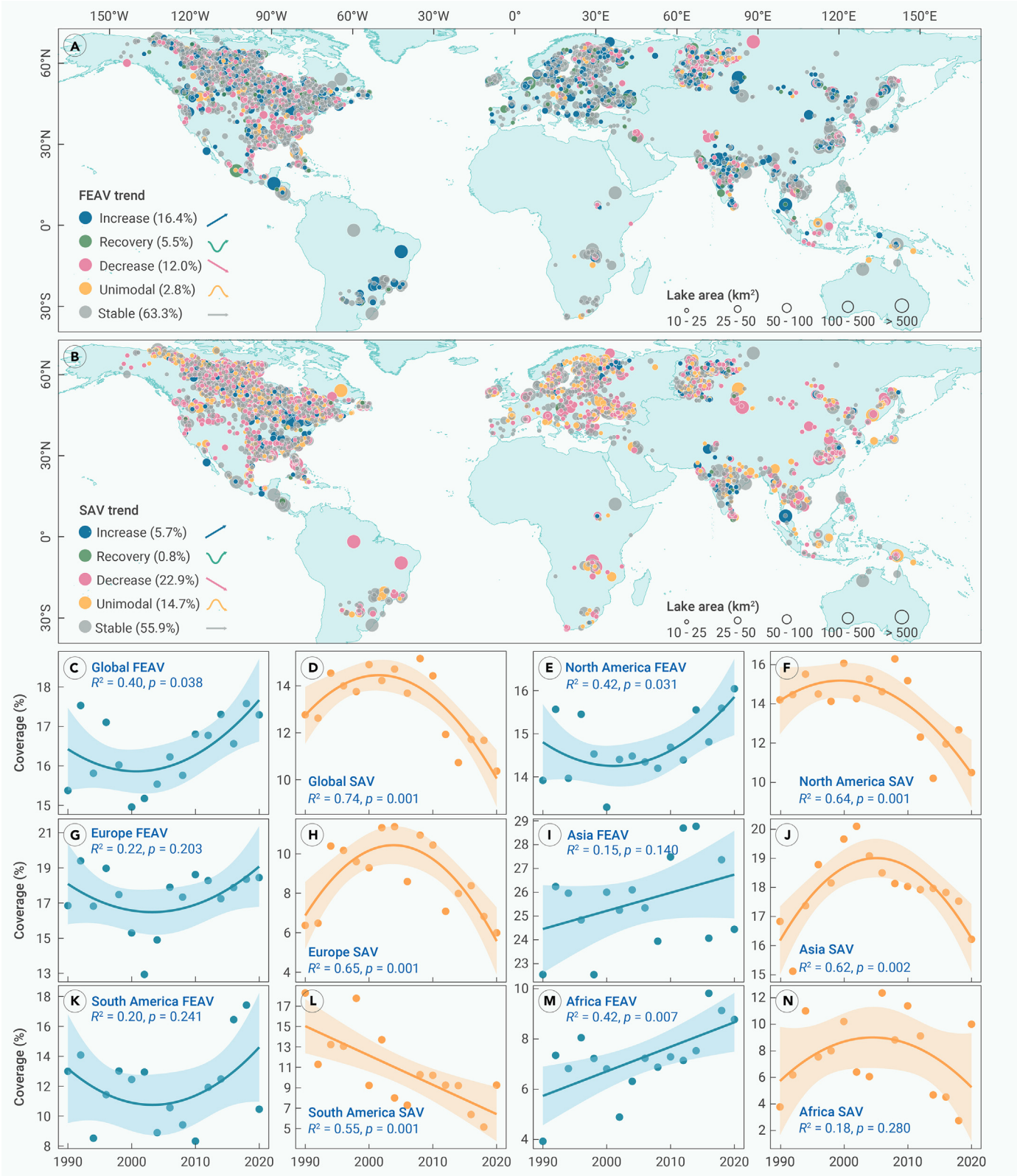

Figure 4. Global trends in lacustrine FEAV and SAV coverage between 1989 and 2021 (A and B) Change patterns of FEAV and SAV in individual lakes. (C) Global FEAV coverage trend (recovery, $p = 0.038$). (D) Global SAV coverage trend (unimodal, $p = 0.001$). (E–N) Evolution patterns of FEAV and SAV coverage across different continents. The y axes in (C)–(N) represents the ratio of total FEAV or SAV area to the area of all lakes in the respective region.

To elucidate the changing dynamics, linear regression analyses were applied to the four influencing factors across the three stages, yielding their respective rates of change. For visual representation, the annual time series for η and the four factors in each region were normalized, considering long-term means and standard deviations to calculate Z scores for factor analysis.

RESULTS

Global patterns of lacustrine AV

Over the past three decades, AV covered an average of 108,186 km^2 globally, accounting for 28.9% (FEAV, 15.8%; SAV, 13.1%) of the total lake area (Figure 3). As of 2020–2021, AV covered 103,090 km^2 (27.6%) (Figure S6). The Northern

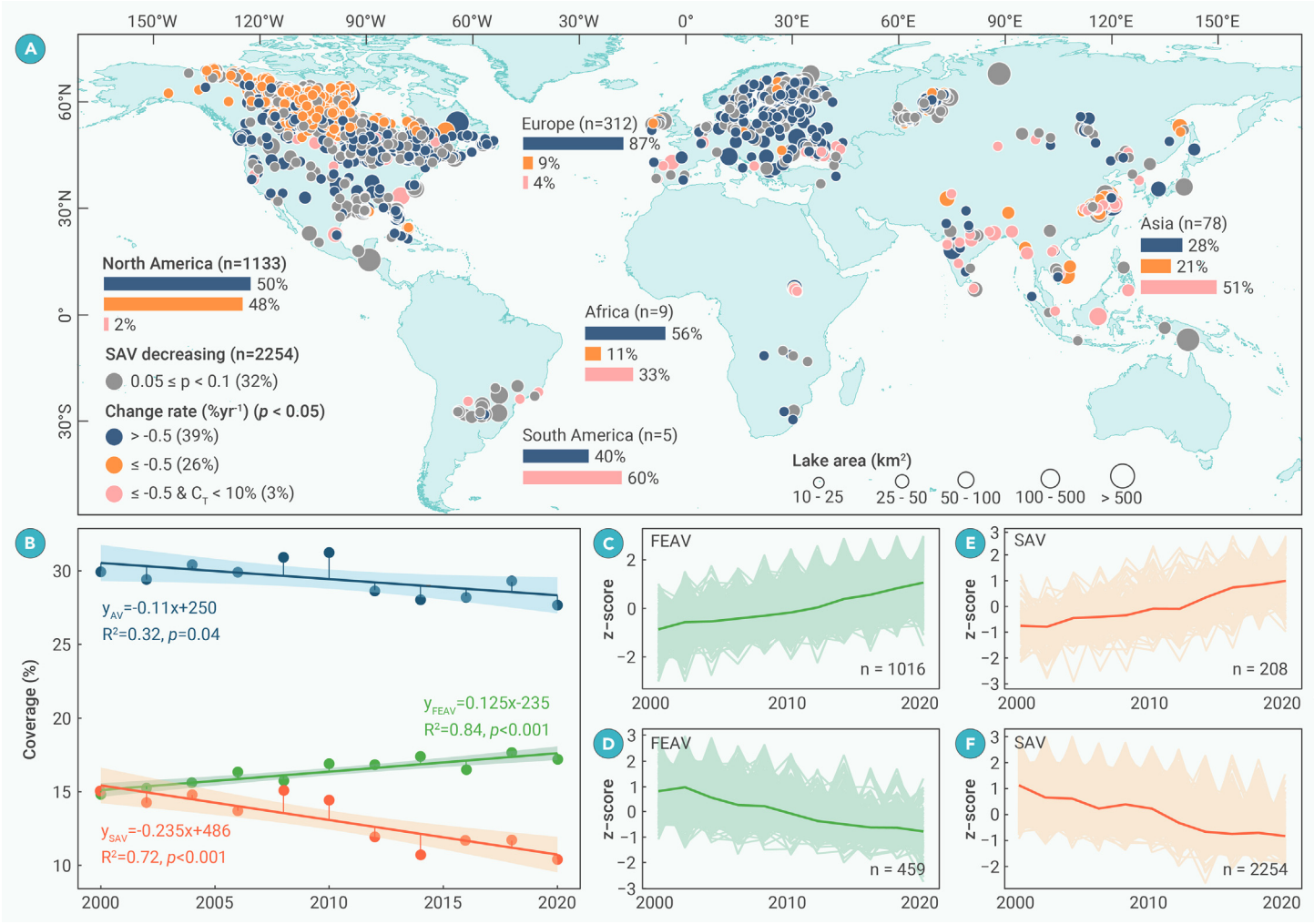

Figure 5. Decline of SAV coverage to varying degrees globally from 2000 and 2021 (A) Distribution of lakes experiencing a decline in SAV. Each point represents one lake with significant decreasing trend of SAV ($p < 0.1$). Red points indicate lakes with a remarkable reduction of SAV, where SAV was nearly absent in the final period. (B) Historical trends of AV (blue), FEAV (green), and SAV (red) coverage from 2000 to 2020 are represented by fitting lines. (C–F) FEAV and SAV coverage histories follow increasing and decreasing trends. The time series of FEAV and SAV coverage *Z* score for each lake is calculated using its own historical mean and standard deviation.

Hemisphere, including North America (6.3×10^4 km^2), Europe (1.9×10^4 km^2), and Asia (2.0×10^4 km^2), accounted for 94.9% of the total AV area. Among the tested lakes, 62.9% (3,516) experience higher AV coverage than the global average. North America (28.2%) and Europe (25.3%) closely resemble the global AV coverage. Oceania, with only 10 tested lakes, displays the highest coverage at 64.4% (FEAV, 28.9%; SAV, 35.5%). Asia ranks second in AV coverage (41.8%), with 81.1% of the tested lakes (467) exceeding the global average. Particularly noteworthy are the middle and lower reaches of the Yangtze River in China, India, and Southeast Asia, which boast the highest AV coverage globally.

Africa (14.2%) and South America (22.5%) exhibit lower AV coverage compared to other continents (Figure 3A). FEAV dominates the AV communities in 78.6% of the tested lakes. AV coverage displays a stronger correlation with FEAV (R^2 = 0.69) than SAV (R^2 = 0.07), indicating that high AV coverage in most lakes is primarily driven by high FEAV abundance (Figures S7A and S7B). The top 10 countries in terms of AV area are Canada, China, Russia, the US, Finland, India, Brazil, Ukraine, Sweden, and Kazakhstan, collectively accounting for 9.6×10^4 km^2 and 88.7% of the global lake AV area (Figure S8). Among these countries, India exhibits the highest AV coverage (45.8%), followed by China (44.7%) and Sweden (35.2%), with the high AV coverage being predominantly attributed to FEAV.

We find that smaller lakes typically have higher coverage of FEAV, with an average coverage of 30.1% in 3,546 small lakes (10–25 km^2) compared to only 10.0% for 101 large lakes (>500 km^2) (Figures S7C–S7F). Lakes ranging in size from 100 km^2 to 500 km^2 have the highest average coverage of SAV. This pattern may be due to deeper water depths and higher wind exposure in large lakes,[26,27] which create unfavorable conditions for FEAV growth but pose less limitation for SAV.[28–31] Among large lakes (>500 km^2), the highest FEAV coverage is found in Lake Nansi (63.3%) and Lake Dongting (38.3%) in China, Lake Michilcamau (34.0%) in Canada, Lake Murray (32.5%) in Papua New Guinea, and Lake Kentucky (30.1%) in the US. The top 5 lakes with the highest SAV coverage are Lake Cedar (57.8%), Lake Moose (54.2%), Lake Southern Indian (47.7%), and Lake St. Clair (38.6%) in Canada along with Lake Argyle (52.9%) in Australia (Figure S9).

Global trends of lacustrine AV

Overall, both in terms of dominant change types and changes in total coverage, SAV rapidly declined while FEAV gradually increased, resulting in a net loss of AV during the study period. Specifically, we analyzed the coverage of SAV and FEAV in individual lakes from 1989 to 2021 and identified five distinct patterns of change: increase, recovery, decrease, unimodal, and stable (Figures 4A, 4B, and S5). Globally, 36.6% (2,047) and 44.1% (2,462) of the tested lakes exhibited significant changes ($p < 0.1$) in FEAV and SAV, respectively. The dominant change types for FEAV and SAV were increase and decrease, respectively, accounting for 44.7% and 51.9% of lakes with discernible change patterns (Figures 4A and 4B). Similar change patterns were observed across five continents, excluding Oceania (Figures S10 and S11). Oceania was excluded from the change analysis due to the limited tested lakes (10) and their representativeness. Lakes in Asia demonstrated the most significant changes in FEAV, with 58.9% (339) of the 576 tested lakes experiencing changes, half of which showed an increase (45.1%) (Figures 4A and S10). In terms of SAV, Asia (47.4%) and Europe (47.2%) had a highest proportion of lakes with change trends compared to the other three continents. The dominant types of changes identified in Asia were

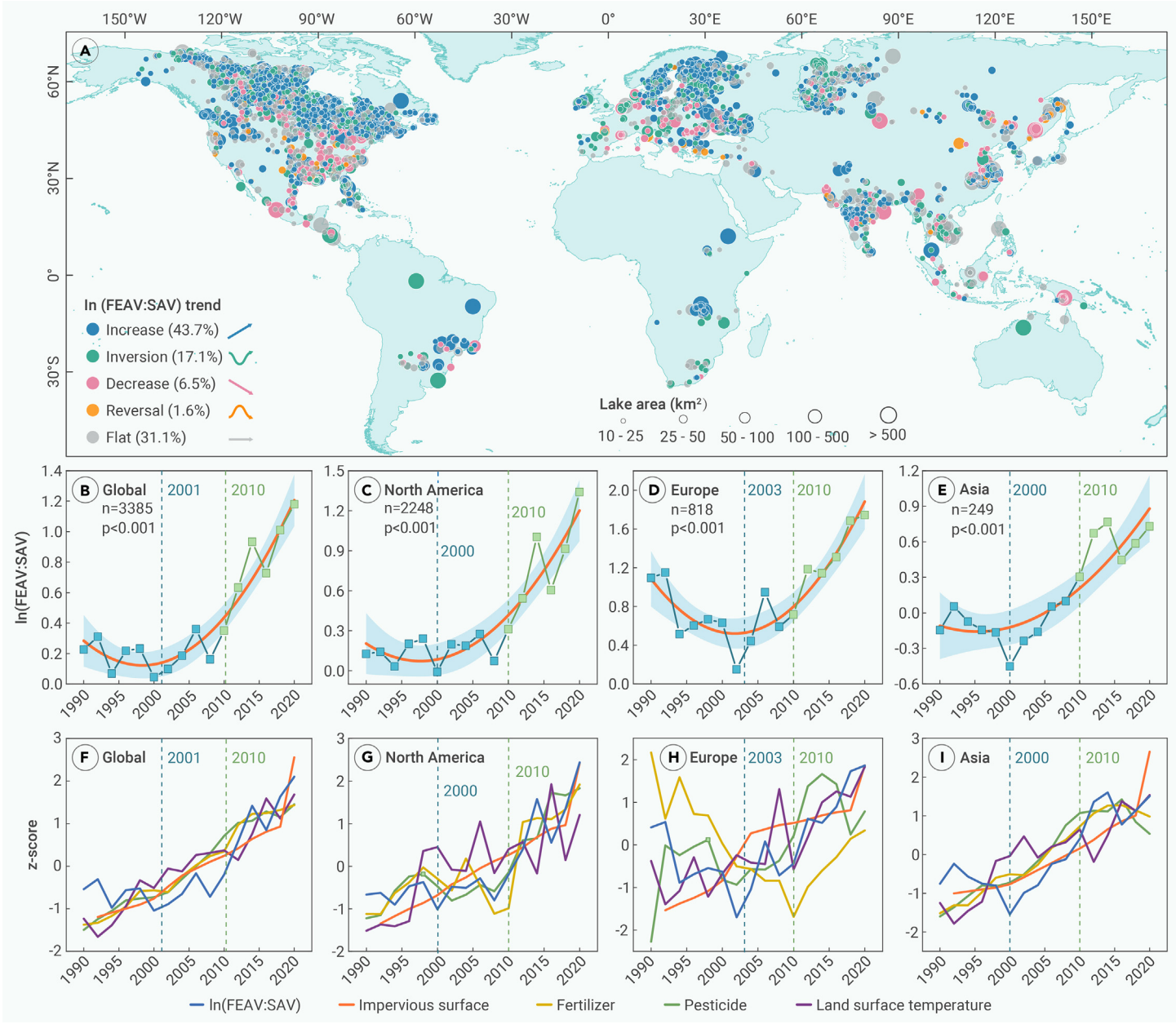

Figure 6. Global trends of η and key factors from 1989 to 2021 (A) η change patterns in individual lakes. (B–E) Change trends of η globally and in North America, Europe, and Asia. (F–I) Two-year moving averages of normalized fertilizer usage, pesticide usage, impervious surface area, and land surface temperature (LST) across continents. The blue and green dashed lines represent the year corresponding to the abrupt change and accelerating increase values of η, respectively.

decrease (52.0%) and unimodal (47.8%) (Figures 4B and S11). Overall, in 34.0% of the lakes, combined AV (FEAV + SAV) displayed significant changes ($p < 0.1$), with a decreasing trend being the dominant change type (44.8%) (Figure S12).

Between 1989 and 2021, there were contrasting change trends in the coverage of FEAV and SAV at the global scale. FEAV displayed a recovery trend ($p = 0.038$; Figure 4C), while SAV exhibited a unimodal trend ($p < 0.001$; Figure 4D). Except for Africa and Asia, where FEAV showed an increasing trend (Figures 4I and 4M), the change trends in coverage for the other three continents aligned with the global trend (Figure 4C). Similarly, except for South America, which demonstrated a significant decreasing trend in SAV (Figure 4L), the remaining four continents exhibited trends consistent with the global trend (Figure 4D). Overall, the total coverage of AV displayed a unimodal trend, aligning with the SAV change trend at global and continental scales (Figures 4D and S11).

Over the past two decades, the changes in SAV and FEAV have been particularly drastic. SAV exhibited a significant decline trend, with a yearly decrease in coverage at an average rate of 0.24% ($p < 0.001$), resulting in a relative decrease of 30.4%. Among the study lakes, 40.3% (2,254 lakes) have shown a decreasing trend in SAV, with 3% of lakes experiencing SAV withering (SAV coverage <10%), primarily observed in the middle and lower reaches of the Yangtze River in China and India (Figure 5A). In contrast, FEAV has exhibited a notable increase over the same period, with an annual growth rate of 0.13% ($p < 0.001$) and an increase of 15.6% from 2000 to 2021. However, despite the increase in FEAV, there has been an overall loss of AV ($p = 0.04$; Figure 5B).

Global regime state shifts of lacustrine AV

We introduced η to effectively assess dominance shifts between FEAV and SAV in lakes or regions. An increasing η indicates increased FEAV dominance or decreased SAV dominance and vice versa. Significant changes in η ($p < 0.1$) occurred over the last 30 years in 3,834 lakes (68.6%). Of these, 63.5% exhibited an increasing trend, while 24.8% showed an inversion pattern (i.e., decrease followed by increase), suggesting a global shift toward greater FEAV or reduced SAV dominance (Figure 6). From 1989 to 2021, a notable inversion in η was observed, characterized by an initial modest decline followed by a substantial and rapid upturn ($p < 0.001$). An abrupt change in η of global lakes occurred in 2001, identified by the M-K test, and an accelerating increase occurred after approximately 2010 (Figure 6B). A shift from increasing SAV or

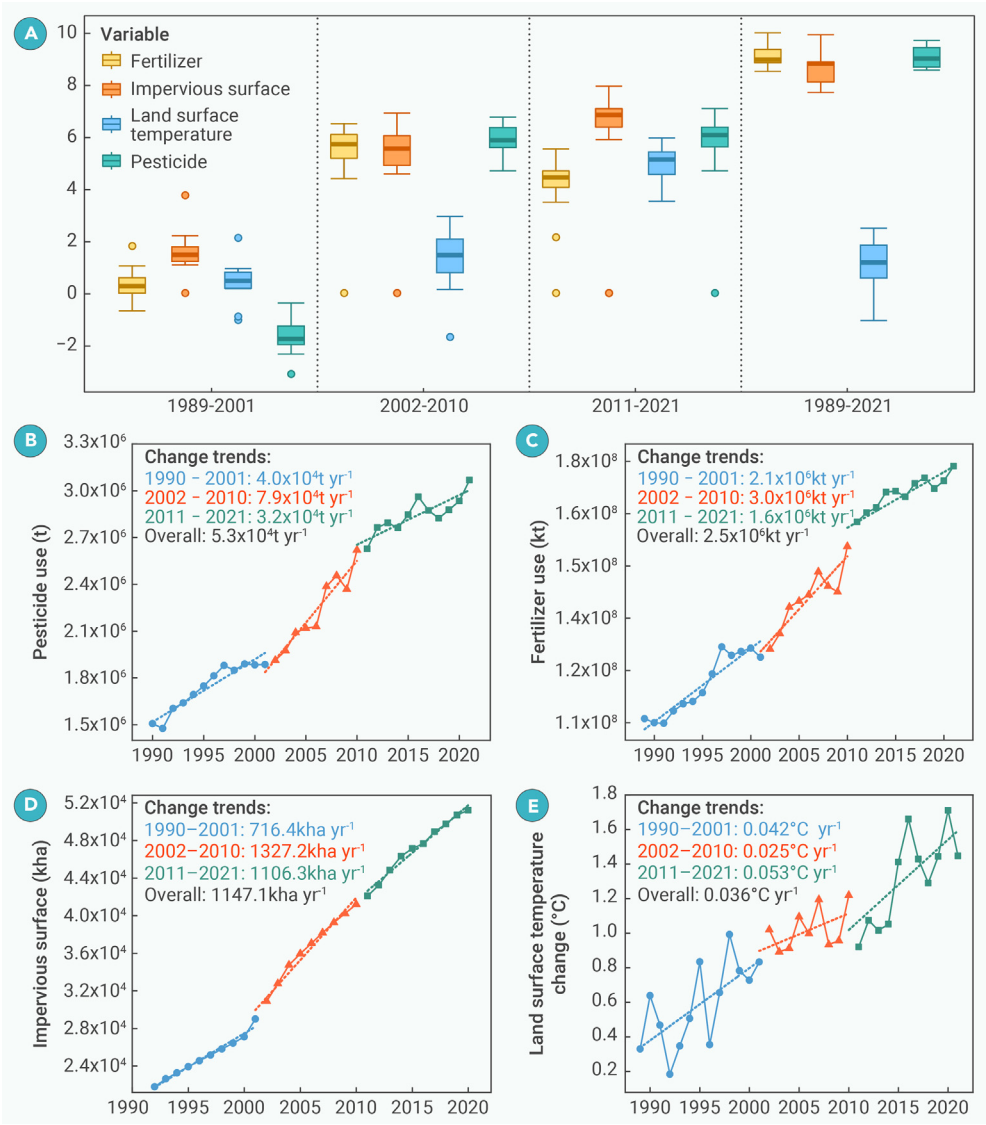

Figure 7. Contributions and long-term change of different factors (A) Contribution of four factors (i.e., fertilizer usage, pesticide usage, expansion of impervious surface and LST change) to the η during the three stages (1989–2001, 2002–2010, and 2011–2021) and overall period. (B–E) Long-term changes in four factors of countries hosting 3,385 lakes. Data are presented in three stages through line charts, and the slopes of trends in different stages are annotated.

decreasing FEAV dominance to increasing FEAV or decreasing SAV dominance occurred since 2001. This trend has become more pronounced after 2010, indicating a potential regime state shift from SAV to FEAV dominance or even AB dominance. Similar trends were observed in major continents, such as North America, Europe, and Asia, where η change trends and accelerating increase years aligned with the global trend, although the years with abrupt change points of η varied (Figures 6C–6E). In 550 of these lakes, SAV exhibited a decrease or unimodal trend, while FEAV exhibited an increase or recovery (Figure S13). This resulted in an increase or reversal of η, indicating a transition toward a shaded state dominated by FEAV. The specific year of abrupt change on η varied across continents and across lakes. For instance, we observed that Lake Changdang in the Yangtze River Basin, China, experienced a shift from an SAV-dominated state to an FEAV-dominated state in 2005 (Figure S14).

Our findings suggest that the decline in global SAV and the increase in FEAV, as well as the resulting increase in η, are closely linked to intense human activities and climatic warming. Prior to 2010, human-induced eutrophication served as the primary driver of change, while the influence of global warming and the consequent rise in lake temperatures likely contributed thereafter. Consistent changes exist between η and some indicators of human activity, such as fertilizer and pesticide usage, as well as impervious surface area. Climate warming indicators, like LST, also show a correlation with η at both global and continental scales (Figures 6F–6I). The impact of human activities outweighs that of climate warming, particularly in North America and Asia (Figure 7A; Table S5). Concurrently, rising temperatures and eutrophication resulting from human activities enhance phytoplankton and FEAV dominance over SAV, potentially triggering a transition.[8,13,32–35] Notably, eutrophication can have a nonlinear effect on SAV coverage, with oligotrophic to mesotrophic lakes experiencing an initial increase in SAV with moderate nutrient additions followed by declines at higher trophic status due to light limitation.[1,36–38] In contrast, FEAV is not light limited and can thrive in high nutrient concentrations.[8,39] In oligotrophic and mesotrophic states, shallow lakes are typically dominated by various SAV, whereas in more eutrophic states, either FEAV or phytoplankton may prevail.[5]

This largely explains the decline in SAV and the increasing trend in FEAV, resulting in a continuous rise in η since 2000. The identified critical years reflect the combined impact of human activities and global warming. Specifically, the period from 2002 to 2010 saw a notable acceleration in human activities, including pesticide and fertilizer use and the expansion of impervious surfaces globally, likely contributing to the observed shift in dominance that occurred in 2001 (Figure 7). Although the rate of increase in human activities slowed after 2010 compared to the period from 2002 to 2010, the rate of increase in LST was twice as high, suggesting that global warming has likely contributed to the rapid rise in η since 2010 (Figure 7).

Future implications

Our findings provide compelling evidence of increased dominance of FEAV and decreased coverage of SAV in lakes on a global scale (Figure 4). Consequently, the index η has been steadily increasing both regionally and globally since 2001 (Figure 5B). Notably, we identified 550 lakes worldwide where SAV decreased while FEAV increased simultaneously (Figure S13). This suggests a growing risk of transitions in lacustrine ecosystems toward a shaded state dominated by FEAV, which can eventually lead to turbid phytoplankton-dominated states under high nutrient loads.[5,11,40,41] Lake Changdang serves as a compelling example of shifting from a clear state dominated by SAV to a shaded state and eventually a turbid state. Prior to 2005, the lake was predominantly covered by SAV, but from 2005 to 2015, SAV decreased while FEAV increased, and frequent ABs occurred thereafter (Figure S14). Such transitions toward phytoplankton-dominated states may be widespread. For instance, more than 8.8% of lakes (>0.1 km^2) worldwide have experienced ABs, and the risk of blooms has increased since 2000.[16] Once a lake transitions to a turbid state, recovery to its original clear state becomes challenging[4,8,42] though possible.[13] This transition is accompanied by a decline in taxonomic and functional diversities while nutrient availability increases, leading to ecological degradation, economic losses, and threats to drinking water safety.[10,43,44]

Our study provides a sign of global shallow lakes transitioning toward shaded or turbid states. The shaded state is transitional, and interrupting FEAV dominance often results in a shift toward a turbid state dominated by phytoplankton, particularly under high nutrient loads. Conversely, removing FEAV can reverse the shift and restore a clear SAV-dominated state, especially under low nutrient loads.[8,42,45] Therefore, slowing down these trends and restoring SAV are currently a priority. Effective management of lake eutrophication is crucial in achieving this goal.[38,46,47] Notably, Europe and China have implemented strong

water restoration policies, such as the European Water Framework Directive adopted in 2000, the Action Plan for Prevention and Control of Water Pollution since 2015, and the Yangtze River Protection Strategy initiated in 2016. However, not all restoration measures have been successful, with cases showing an increase in FEAV rather than SAV.[24] If nutrient levels are sufficiently reduced, then a one-time removal of floating plants could tip the balance toward an alternative state dominated by SAV.[45] Therefore, maintaining or recovering SAV through global collaborative efforts is needed, including reducing nutrient loading from agricultural areas, aquaculture, and urban sources as well as implementing SAV restoration and FEAV harvesting when needed.[48–51]

CONCLUSION

In this study, we established a global AV database by leveraging 1.4 million Landsat images from 1989 to 2021 with the aim of attaining a comprehensive understanding of the ecosystems within 5,587 shallow lakes. The average AV coverage was calculated as 28.9%, encompassing an area of 108,186 km^2, predominantly distributed across North America, Europe, and Asia. Our findings suggest that SAV is undergoing a significant decline, whereas FEAV is experiencing a gradual increase, thereby suggesting a regime shift from clear to shaded or even turbid states. Until the early 2010s, human activities predominantly drove the global trends; however, climate warming has since become the dominant driver shaping changes in lake ecosystems. Our innovative methodology and the established database present a potent instrument for real-time monitoring and a more profound global understanding of lake ecosystems, bearing substantial implications for lake management and global conservation initiatives.

DATA AND CODE AVAILABILITY

- The Landsat images are available in the data archive of GEE: https://developers.google.com/earth-engine/datasets.
- The HydroLAKES dataset was obtained at https://www.hydrosheds.org/pages/hydrolakes.
- The endorheic basin polygons were downloaded from https://doi.org/10.1594/PANGAEA.895895?format=html#.
- The global temperature data are available in the data archive of GEE: https://developers.google.com/earth-engine/datasets/catalog/ECMWF_ERA5_LAND_MONTHLY_AGGR.
- The data series of fertilizer usage, impervious surface area, and LST changes were obtained from the FAO: https://www.fao.org/faostat.
- The global lacustrine AV database is available from the corresponding author upon reasonable request.

REFERENCES

1. Botrel, M. and Maranger, R. (2023). Global historical trends and drivers of submerged aquatic vegetation quantities in lakes. *Global Change Biol.* **29**:2493–2509.
2. Pan, Y., García-Girón, J. and Iversen, L.L. (2023). Global change and plant-ecosystem functioning in freshwaters. *Trends Plant Sci.* **28**:646–660.
3. Rosentreter, J.A., Laruelle, G.G. and Bange, H.W. (2023). Coastal vegetation and estuaries are collectively a greenhouse gas sink. *Nat. Clim. Change* **13**:579–587.
4. Hilt, S., Jeppesen, E. and Veraart, A.J. (2017). Translating Regime Shifts in Shallow Lakes into Changes in Ecosystem Functions and Services. *Bioscience* **67**:928–936.
5. van Wijk, D., Chang, M., Janssen, A.B.G. et al. (2023). Regime shifts in shallow lakes explained by critical turbidity. *Water Res.* **242**:119950. DOI:https://doi.org/10.1016/j.watres.2023.119950.
6. Amorim, C.A. and Moura, A.N. (2020). Effects of the manipulation of submerged macrophytes, large zooplankton, and nutrients on a cyanobacterial bloom: A mesocosm study in a tropical shallow reservoir. *Environ. Pollut.* **265**:114997. DOI:https://doi.org/10.1016/j.envpol.2020.114997.
7. Moss, B. (1990). Engineering and biological approaches to the restoration from eutrophication of shallow lakes in which aquatic plant communities are important components. *Hydrobiologia* **200–201**:367–377.
8. De Tezanos Pinto, P. and O'Farrell, I. (2014). Regime shifts between free-floating plants and phytoplankton: a review. *Hydrobiologia* **740**:13–24.
9. Luo, J., Li, X., Ma, R. et al. (2016). Applying remote sensing techniques to monitoring seasonal and interannual changes of aquatic vegetation in Taihu Lake, China. *Ecol. Indicat.* **60**:503–513.
10. Moi, D.A., Romero, G.Q., Jeppesen, E. et al. (2022). Regime shifts in a shallow lake over 12 years: Consequences for taxonomic and functional diversities, and ecosystem multifunctionality. *J. Anim. Ecol.* **91**:551–565.
11. Janssen, A.B.G., Hilt, S., Kosten, S. et al. (2020). Shifting states, shifting services: Linking regime shifts to changes in ecosystem services of shallow lakes. *Freshw. Biol.* **66**:1–12.
12. Scheffer, M., Szabo, S., Gragnani, A. et al. (2003). Floating plant dominance as a stable state. *Proc. Natl. Acad. Sci. USA* **100**:4040–4045.
13. Meerhoff, M. and Jeppesen, E. (2024). Shallow Lakes and Ponds. In Environmental Science (Elsevier), pp. 859–892. DOI:https://doi.org/10.1016/B978-012370626-3.00041-7.
14. Spears, B.M., Futter, M.N., Jeppesen, E. et al. (2017). Ecological resilience in lakes and the conjunction fallacy. *Nat. Ecol. Evol.* **1**:1616–1624.
15. Ho, J.C., Michalak, A.M. and Pahlevan, N. (2019). Widespread global increase in intense lake phytoplankton blooms since the 1980s. *Nature* **574**:667–670.
16. Hou, X., Feng, L., Dai, Y. et al. (2022). Global mapping reveals increase in lacustrine algal blooms over the past decade. *Nat. Geosci.* **15**:130–134.
17. Wang, S., Li, J., Zhang, B. et al. (2018). Trophic state assessment of global inland waters using a MODIS-derived Forel-Ule index. *Rem. Sens. Environ.* **217**:444–460.
18. Dai, Y., Feng, L., Hou, X. et al. (2021). An automatic classification algorithm for submerged aquatic vegetation in shallow lakes using Landsat imagery. *Rem. Sens. Environ.* **260**:112459. DOI:https://doi.org/10.1016/j.rse.2021.112459.
19. Luo, J., Ni, G., Zhang, Y. et al. (2023). A new technique for quantifying algal bloom, floating/emergent and submerged vegetation in eutrophic shallow lakes using Landsat imagery. *Rem. Sens. Environ.* **287**:113480. DOI:https://doi.org/10.1016/j.rse.2023.113480.
20. Piaser, E. and Villa, P. (2023). Evaluating capabilities of machine learning algorithms for aquatic vegetation classification in temperate wetlands using multi-temporal Sentinel-2 data. *Int. J. Appl. Earth Obs. Geoinf.* **117**:103202. DOI:https://doi.org/10.1016/j.jag.2023.103202.
21. Messager, M.L., Lehner, B., Grill, G. et al. (2016). Estimating the volume and age of water stored in global lakes using a geo-statistical approach. *Nat. Commun.* **7**:13603. DOI:https://doi.org/10.1038/ncomms13603.
22. Ma, R., Yang, G., Duan, H. et al. (2011). China's lakes at present: Number, area and spatial distribution. *Sci. China Earth Sci.* **54**:283–289.
23. Wang, J.D., Song, C.Q., Reager, J.T. et al. (2018). Recent global decline in endorheic basin water storages. *Nature geoscience* **11**:926–932. DOI:https://doi.org/10.1594/PANGAEA.895895.
24. Zhang, Y., Jeppesen, E., Liu, X. et al. (2017). Global loss of aquatic vegetation in lakes. *Earth Sci. Rev.* **173**:259–265.
25. Liu, N.N., Jiao, N., Tan, J.C. et al. (2022). Multi-kingdom microbiota analyses identify bacterial–fungal interactions and biomarkers of colorectal cancer across cohorts. *Nat. Microbiol.* **7**:238–250.
26. Gorham, E. and Boyce, F.M. (1989). Influence of lake surface area and depth upon thermal stratification and the depth of the summer thermocline. *J. Great Lake. Res.* **15**:233–245.
27. Cael, B.B. and Seekell, D. (2022). A theory for the relationship between lake surface area and maximum depth. *Limnol. Oceanogr. Lett.* **7**:527–533.
28. Deegan, B.M., White, S.D. and Ganf, G.G. (2007). The influence of water level fluctuations on the growth of four emergent macrophyte species. *Aquat. Bot.* **86**:309–315.
29. Schneider, B., Cunha, E.R., Marchese, M. et al. (2018). Associations between macrophyte life forms and environmental and morphometric factors in a large sub-tropical floodplain. *Front. Plant Sci.* **9**:195. DOI:https://doi.org/10.3389/fpls.2018.00195.
30. Strand, J.A. and Weisner, S.E.B. (2001). Morphological plastic responses to water depth and wave exposure in an aquatic plant (Myriophyllum spicatum). *J. Ecol.* **89**:166–175.
31. Zhou, J., Leavitt, P.R., Zhang, Y. et al. (2022). Anthropogenic eutrophication of shallow lakes: Is it occasional? *Water Res.* **221**:118728. DOI:https://doi.org/10.1016/j.watres.2022.118728.
32. Huang, F., Zhang, K., Huang, S. et al. (2021). Patterns and trajectories of macrophyte change in East China's shallow lakes over the past one century. *Sci. China Earth Sci.* **64**:1735–1745.
33. Meerhoff, M. and Beklioğlu, M. (2024). Shallow lakes and ponds. In Wetzel's Limnology (Elsevier), pp. 859–892. DOI:https://doi.org/10.1016/B978-0-12-822701-5.00026-4.
34. Grant, L., Vanderkelen, I., Gudmundsson, L. et al. (2021). Attribution of global lake systems change to anthropogenic forcing. *Nat. Geosci.* **14**:849–854.
35. Capon, S.J., Lynch, A.J.J., Bond, N. et al. (2015). Regime shifts, thresholds and multiple stable states in freshwater ecosystems; a critical appraisal of the evidence. *Sci. Total Environ.* **534**:122–130.
36. Vermaire, J.C. and Gregory-Eaves, I. (2008). Reconstructing changes in macrophyte cover in lakes across the northeastern United States based on sedimentary diatom assemblages. *J. Paleolimnol.* **39**:477–490.
37. Zhang, Y., Qin, B., Shi, K. et al. (2020). Radiation dimming and decreasing water clarity fuel underwater darkening in lakes. *Sci. Bull.* **65**:1675–1684.
38. Xu, X., Zhang, Y., Chen, Q. et al. (2020). Regime shifts in shallow lakes observed by remote sensing and the implications for management. *Ecol. Indicat.* **113**:106285. DOI:https://doi.org/10.1016/j.ecolind.2020.106285.
39. Ersoy, Z., Scharfenberger, U., Baho, D.L. et al. (2020). Impact of nutrients and water level changes on submerged macrophytes along a temperature gradient: A pan-European mesocosm experiment. *Global Change Biol* **26**:6831–6851.
40. Dong, B., Zhou, Y., Jeppesen, E. et al. (2022). Six decades of field observations reveal how anthropogenic pressure changes the coverage and community of submerged aquatic vegetation in a eutrophic lake. *Sci. Total Environ.* **842**:156878. DOI:https://doi.org/10.1016/j.scitotenv.2022.156878.
41. Chao, C., Lv, T., Wang, L. et al. (2022). The spatiotemporal characteristics of water quality and phytoplankton community in a shallow eutrophic lake: Implications for submerged vegetation restoration. *Sci. Total Environ.* **821**:153460. DOI:https://doi.org/10.1016/j.scitotenv.2022.153460.
42. Scheffer, M. and Van Nes, E.H. (2007). Shallow lakes theory revisited: various alternative regimes driven by climate, nutrients, depth and lake size. *Hydrobiologia* **584**:455–466.
43. Weyhenmeyer, G.A., Chukwuka, A.V., Anneville, O. et al. (2024). Global Lake Health in the Anthropocene: Societal Implications and Treatment Strategies. *Earth's Future* **12**:e2023EF004387. DOI:https://doi.org/10.1029/2023EF004387.

44. Rohr, J.R., Sack, A., Bakhoum, S. et al. (2023). A planetary health innovation for disease, food and water challenges in Africa. *Nature* **619**:782–787.
45. Scheffer, M. and Carpenter, S.R. (2003). Catastrophic regime shifts in ecosystems: linking theory to observation. *Trends Ecol. Evol.* **18**:648–656.
46. Wang, D., Gan, X., Wang, Z. et al. (2023). Research status on remediation of eutrophic water by submerged macrophytes: A review. *Process Saf. Environ. Protect.* **169**:671–684.
47. Bakker, E.S., Sarneel, J.M., Gulati, R.D. et al. (2013). Restoring macrophyte diversity in shallow temperate lakes: biotic versus abiotic constraints. *Hydrobiologia* **710**:23–37.
48. Hallegraeff, G.M., Anderson, D.M., Belin, C. et al. (2021). Perceived global increase in algal blooms is attributable to intensified monitoring and emerging bloom impacts. *Commun. Earth Environ.* **2**:117.
49. Gremmen, T., van Dijk, G., Postma, J. et al. (2023). Factors influencing submerged macrophyte presence in fresh and brackish eutrophic waters and their impact on carbon emissions. *Aquat. Bot.* **187**:103645. DOI:https://doi.org/10.1016/j.aquabot.2023.103645.
50. Luo, J., Pu, R., Duan, H. et al. (2020). Evaluating the influences of harvesting activity and eutrophication on loss of aquatic vegetations in Taihu Lake, China. *Int. J. Appl. Earth Obs. Geoinf.* **87**:102038. DOI:https://doi.org/10.1016/j.jag.2019.102038.
51. Liu, Z., Hu, J., Zhong, P. et al. (2018). Successful restoration of a tropical shallow eutrophic lake: Strong bottom-up but weak top-down effects recorded. *Water Res.* **146**:88–97.

ACKNOWLEDGMENTS

We thank NASA for providing global Landsat satellite images. This research was supported by the National Natural Science Foundation of China (42425104, 42271377, and 42271114), the Key Laboratory of Lake and Watershed Science for Water Security (NKL2023-KP02 and NIGLAS2022GS09), the PIFI Project of the Chinese Academy of Sciences (2024PG0017 and 2024DC0005), the International Research Center of Big Data for Sustainable Development Goals (CBAS) (CBASYX0906), the TÜBITAK program BIDEB2232 (118C250), the UKRI Natural Environment Research Council (NERC) Independent Research Fellowship (NE/T011246/1), and the UK EO Climate Information Service (NE/X019071/1). The funders had no role in study design, data collection and analysis, decision to publish, or preparation of the manuscript. We thank Z. Cao, Z. Sun, J. Ma, Y. Dai, and X. Hou for discussions and input and Anne Mette Poulsen for valuable English editions.

AUTHOR CONTRIBUTIONS

J.L. and H.D., conceptualization, methodology, funding acquisition, supervision, and writing; Y. Xu, M.S., G.N., K.W., Y. Xin, and T.Q., data processing and analyses; Y.Z., conceptualization and refinement of the manuscript. Q.X., L.F., Y.Q., E.J., and R.I.W. participated in interpreting the results and refining the manuscript. All authors contributed to and approved the manuscript.

DECLARATION OF INTERESTS

The authors declare no competing interests.

SUPPLEMENTAL INFORMATION

It can be found online at https://doi.org/10.1016/j.xinn.2024.100784.

LEAD CONTACT WEBSITE

https://niglas.cas.cn/yjsjy_165790/dsjs/bshshdsh/dtxydlxxxt/202005/t20200509_5577094.html

https://niglas.cas.cn/yjsjy_165790/dsjs/bshshdsh/hjkx/202005/t20200509_5577111.html.